

Whole-exome Sequencing Reveals the Etiology of the Rare Primary Hepatic Mucoepidermoid Carcinoma

Ping Hou

Nanchang University Second Affiliated Hospital

Xiaoyan Su

Nanchang University Second Affiliated Hospital

Wei Cao

Nanchang University First Affiliated Hospital

Liping Xu

Nanchang university third affiliated hospital

Rongguiyi Zhang

Nanchang University Second Affiliated Hospital

Zhihao Huang

Nanchang University Second Affiliated Hospital

Jiakun Wang

Nanchang University Second Affiliated Hospital

Lixiang Li

Nanchang University Second Affiliated Hospital

Linqun Wu

Nanchang University Second Affiliated Hospital

Wenjun Liao (✉ liaowenjun120@163.com)

Nanchang University Second Affiliated Hospital

Research

Keywords: hepatic mucoepidermoid carcinoma (HMEC), somatic GNAS R201 mutation, germline Fanconi Anemia mutation, whole exome-sequencing (WES)

Posted Date: November 2nd, 2020

DOI: <https://doi.org/10.21203/rs.3.rs-99715/v1>

License:  This work is licensed under a Creative Commons Attribution 4.0 International License. [Read Full License](#)

Version of Record: A version of this preprint was published at Diagnostic Pathology on April 8th, 2021. See the published version at <https://doi.org/10.1186/s13000-021-01086-3>.

Abstract

Background Primary hepatic mucoepidermoid carcinoma (HMEC) is extremely rare and the molecular etiology is still unknown. Recently, The *CRTC1-MAML2* fusion gene was detected in a primary HMEC which is often associated with MEC of salivary gland in the literature.

Methods a 64-year-old male was diagnosed with HMEC based on malignant squamous cells and mucus-secreting cells in immunohistochemical examination. Whole-exome sequencing (WES) and sanger sequencing were used to reveal the molecular characteristics of HMEC, and analysis with public data among hepatocellular carcinoma, cholangiocarcinoma and salivary MEC. Meanwhile, The susceptibility genes were identified in pedigree investigation.

Result Significant somatic mutations in *GNAS*, *KMT2C*, *ELF3* genes were identified in primary HMEC by WES and sanger sequencing. Meanwhile, through public data analysis, somatic *GNAS* gene altered in 2.1% hepatobiliary tumors, and typically *GNAS* occur at exon 8, in which Arg201 is converted to either a cysteine (R201C) or a histidine (R201H) related with cholangiocarcinoma associated with parasite infection. Furthermore, heterozygous germline mutations of *FANCA*, *FANCI*, *FANCI/BRIP1* and *FAN1* genes were also identified. Pedigree investigation verified that mutation of susceptibility genes of Fanconi's anemia were present in the pedigree.

Conclusions It was the first time to demonstrate the molecular etiology of the rare HMEC associated with germline Fanconi's anemia mutations and somatic *GNAS* R201H mutation.

Background

Mucoepidermoid carcinoma (MEC) is a relatively common malignant neoplasm of salivary gland and mainly characterized by the pathological manifestation of mucous cells, intermediate cells and epidermoid malignant cells in intimately mixed nest. However, MEC rarely occurs at other sites of the body like the esophagus, thyroid gland, lacrimal gland, lung, thymus, breast, anal canal, uterine cervix, hepatobiliary and pancreatic system¹. Over 50–60% of salivary mucoepidermoid carcinoma (SMEC) are associated with a fusion gene, *CRTC1/CRTC3-MAML2*, which results from the chromosomal translocation $t(11;19)(q21;p13)$ ². The *CRTC1-MAML2* fusion gene was also observed in primary cervical MEC³ and bronchopulmonary MEC⁴, which are different from adenocarcinoma. However, pancreatic MEC did not show the *CRTC1/3-MAML2* fusion and were a morphologic variant of pancreatic adenocarcinoma⁵. While it was controversy whether the *CRTC1-MAML2* fusion gene was detected in primary hepatic MEC^{6, 7}. Otherwise, MEC was also associated with hematopoietic stem-cell transplant in Fanconi anemia patients⁸. So far, only 23 cases with primary hepatobiliary MEC (including hepatic, biliary and gall bladder MEC) that were pathomorphologically similar to SMEC have been reported in literatures (Table 1), but the molecular etiology of HMEC is still unknown. Here we revealed the genetic abnormality of a primary hepatic MEC by whole-exome sequencing (WES).

Table 1

Basic characteristics of 23 patients with primary hepatobiliary(including in the liver,gallbladder,biliary tract) mucoepidermoid carcinoma reported in literature

Case	Year	Area	Age (year)	Gender	Location	Metastasis	Size (cm)	Hepatitis	AFP ng/ml	CA199 u/ml	CEA ng/ml	Treatment	OS (day)	Referen
1	1971	Argentina	44	M	RL	Non	15	Np	Np	Np	Np	S	45	
2	1980	Hong Kong	65	M	RL	Y	8	Np	Np	Np	Np	Con	14	
3		Hong Kong	63	F	LL	Y	6	Np	Np	Np	Np	Con	16	
4	1982	Hong Kong	44	F	LL	Non	12	HBV	Np	Np	Np	S + C	180	33
5		Hong Kong	66	M	BD	Y	4	Non	Np	Np	Np	PTCD + S	7	
6		Hong Kong	62	M	BD	Non	1.5	Non	Np	Np	Np	S	300+	
7	1984	Japan	78	M	LL	Y	11	Np	12.5	Np	1300	C	90	28
8	1986	Krean	35	M	LL	Non	18	Np	< 5	Np	Np	Con	14	
9	1986	Australia	59	F	RL	Y	18	Np	Np	Np	Np	S	14	
10	1987	Japan	46	F	LL	Non	3	Np	20	Np	Np	S	330	18
11	1992	Italy	66	F	LL	Y	9.5	Non	< 5	500	< 2	S	180	27
12	1994	Krean	68	M	LL	Non	10	Np	Np	Np	Np	TACE + C	1095	
13	2000	Thailand	64	M	LL	Y	5	Np	Np	Np	Np	Con	210	
14	2003	Krean	52	M	LL	Y	7	Np	< 5	400	Np	S	180	16
15	2004	Krean	69	F	RL	Y	16	Non	< 5	240	Np	S	120	
16	2008	Japan	81	F	RL	Y	10	Non	< 5	14893	Np	C	117	
17	2011	Krean	70	M	BD	Y	8	HCV	< 5	349	Np	R + C	106	
18	2012	Japan	68	M	BD	Y	5	Non	Np	50.8	Np	S + R + C	90+	17
19	2013	America	83	F	BD	Y	2	Np	Np	940	10	S + C	390	7
20	2014	China	60	F	LL	Y	8.5	Non	< 5	50	Np	S + R	180	
21	2019	India	50	M	GB	Y	8	Non	< 5	652	77	S	180	1
22	2019	Japan	79	F	RL	Y	4	Non	< 5	415	146	S + R + C	3650+	6
23	2020	China	60	M	LL	Non	13	Non	< 5	151	10	S	90	presen

Abbreviation Non: not have **Np:**not provided,**RL:**right liver,**LL:**left liver,**BD:** bile duct,**GB:**gallbladder,**HCC:**Hepatocellular carcinoma,**S;**surgery,**R:**Radiotherapy,**C:**Chemotherapy,**Con:**Conservative,**TACE:**transcatheter arterial chemoembolization.**PTCD:**percutaneous transhepatic cholangial drainage.**OS:**overall survival.

Methods And Case Material

A 64-year-old male was admitted to the Second Affiliated Hospital of Nanchang University on September 16, 2019 with a complaint of repeated abdominal distension over a period of one year. He had a previous history of icteric hepatitis and unknown biliary tract surgery 30 years prior and coronary artery stenosis disease with an implanted stent one year ago. No special abnormality was found in the physical examination. Most preoperative laboratory tests were in the normal range, including serum glutamic pyruvic transaminase, glutamic oxaloacetic transaminase, total bilirubin, electrolyte, glucose and platelet count, and serum alpha fetoprotein level. Hepatitis B surface antigen and hepatitis C antibody were both negative. Abnormal blood test results included C-reactive protein 112.3 mg/l (normal value, < 10 g/l), white blood cell $9.82 \times 10^9/l$ (normal value, $3.5-9.5 \times 10^9/l$), red blood cell 3.68×10^9 (normal value, $4.3-5.8 \times 10^9/l$), hemoglobin 103 g/l (normal value 130–175 g/l), alkaline phosphatase 483.9 U/L (normal value 45–125 U/L), γ -glutamine dehydrogenase 404.84 U/L (normal value 10–60 U/L), carcinoembryonic antigen (CEA) 10.2 ng/mL (normal value, < 5.0 ng/mL) and carbohydrate antigen 19 - 9 (CA19-9) 151.2 U/mL (normal value, < 37 U/mL). Ultrasonography, magnetic resonance imaging and abdominal enhanced computed tomography (CT) revealed a mass lesion measuring approximate 10 cm in diameter at the left hepatic lobe and intrahepatic bile ducts with multiple stones (*Supplementary Fig. 1A.B.C*). The patient underwent resection with left hemihepatectomy and choledocholithotomy and T-tube drainage. Then, the patient was diagnosed with HMEC based on malignant squamous cells and mucus-secreting cells in pathological examination. There was gradually increased jaundice in the postoperative term, and the patient died of hepatic function failure at postoperative three months.

This study was approved by the Ethics Committee of the Second Affiliated Hospital of Nanchang University, and informed consent was obtained from the patient and his family. Parts of tumor tissues and corresponding non-tumor tissues were immediately conserved in a liquid nitrogen tank at -80°C. Some

tissue samples were fixed in 10% formaldehyde and paraffin-embedded for pathological diagnosis and immunohistochemistry. Exome sequencing and Sanger sequencing were performed in fresh tumor tissue and corresponding non-tumor tissue. The WES data from this study were deposited in NCBI Sequence Read Archive under accession SRA:SRP 266690.

Histopathologica examination

Hematoxylin eosin staining were detected for tumor samples and correspondent non-tumor samples. Strictly follow the standard procedure of immunohistochemistry. primary antibody diluted at 1:50. Antibody concluded MUC1 (Servicebio, mouse monoclonal, diluted 1:200), MUC5AC (Servicebio, mouse monoclonal, diluted 1:200), CK7 (Servicebio, mouse monoclonal, diluted 1:200), CK19 (Servicebio, rabbit polyclonal, diluted 1:500), and P63 (Servicebio, rabbit polyclonal, diluted 1:500). CEA (Servicebio, mouse monoclonal, diluted 1:200). Both of the two senior pathology specialists from Affiliated Hospital of NanChang University (XY Su and LP Xu) who examined the results suggested a diagnosis of HMEC.

WES

Exome capture was performed using 0.6 µg genomic DNA per sample. Sequencing libraries were generated using the Agilent SureSelect Human All Exon V6 kit (Agilent Technologies, CA, USA). The DNA libraries were sequenced on an Illumina HiSeq platform and 150 bp paired-end reads were generated. The original fluorescence image files were transformed to raw data by base calling and clean data was in turn recorded in FASTQ format. Valid sequencing data was mapped to the reference human genome (UCSC hg19) by Burrows-Wheeler Aligner software and results were stored in BAM format. Samtools mpileup and bcftools were used to do variant calling and identify single-nucleotide variant (SNV) and InDel. Functional annotation ANNOVAR was performed to do annotation for Variant Call Format and detect variants by 1000 Genome, dbSNP and other databases. Given the significance of exonic variants, gene transcript annotation databases such as Consensus CDS, RefSeq, Ensembl and UCSC were also included to determine amino acid alterations. Based on the paired samples of tumor tissue and corresponding non-tumor tissues, somatic SNVs were detected by MuTect, somatic InDels by Strelka and somatic CNVs by Control-FREEC. Software SIFT, Polyphen/Polyphen2 and MutationAssessor were used to predict the impact of SNV on function; and truncated mutations (nonsense and frameshift) also resulted in high functional impact alterations.

Public datas analysis

The search and analytic strategy was performed using the public Datas (<http://www.cbioportal.org/>)^{9, 10}. SNVs were examined in hepatocellular carcinoma (HCC) and cholangiocarcinoma (CHL). We also downloaded SMEC SNVs¹¹ data from published studies to examine the relation between alternations in the current case with downloaded data. We used an online tool to make Venn diagrams.

Sanger sequencing and Pedigree survey

Purified DNA was isolated from the proband's fresh tumor tissue and corresponding non-tumor tissue and from peripheral blood lymphocytes of four family members using a TIANamp Genomic DNA Kit (Beijing Biotech, China). PCR was performed using the PTC-200PC instrument (BIO-RAD, USA). Primer sequences are shown in *Supplementary table 2*. The PCR products were examined using an ABI 3730XL DNA Analyzer (Applied Biosystems, USA).

Results

Microscopic Features and Immunohistochemistry

The mass was an irregular specimen measuring approximately 10 × 7 × 6 cm, revealing no fibrous capsule and tough solid texture, and resection from the middle edge showed grayish-white nodules without necrosis. Black pigment stones were also found in the small intrahepatic bile duct (*Supplementary Fig. 1D*). The resection edges were free of tumor. There was an absence of cirrhosis in the corresponding non-tumor sample, but massive inflammatory cell infiltration was observed in tumorous and portal areas. Hematoxylin and eosin staining revealed that the tumor cells were composed of epidermoid malignant cells, mucous cells and intermediate cells. Alcian blue staining revealed the mucin in mucin-producing cells. The distribution of epidermoid cell was not nest-like but was surrounded with intercellular bridges, with only a few glandular structures and occasional keratinization. Mucin-producing cells showed mainly abundant clear cytoplasm with eccentric pyknotic nuclei and predominantly showed intracellular mucus and rare extracytoplasmic mucin. The heterogeneity of epidermoid cells was obvious, with infiltrated stroma and invasion, but nerve, lymphovascular, blood invasion and necrosis were not apparent (Fig. 1A, B, C, D). Immunohistochemically, MUC5AC was only positive in the cytoplasm of mucous cells (Fig. 2A). Positive MUC1 was localized to the squamous and mucous tumor cell membrane (Fig. 2B). p63 was diffusely positive in the nuclei of malignant squamoid cells and mucinous cells (Fig. 2C), but cytoplasmic CK7 and CK19 were focal positive (Fig. 2D, E). CEA was negative on all tumor cells (Fig. 2F).

Somatic variants in the proband

The sequencing of tumor tissue and corresponding non-tumor tissue in proband provided average coverage depth on target of 175X and 112X, and >10X coverage of the targeted gene regions were 94% and 98%, respectively. The total somatic variants included 135 SNVs (53 missenses, 31 synonymous, 3 nonsense and others) and 4 InDels (2 frameshift insertions and 2 frameshift deletions). A total of 252 copy number variants (CNVs) (126 gain, 126 loss) were identified in 2591 genes (629 gene gain, 1691 gene loss). GNAS mutation (NM_000516:exon8:c.G602A:p.R201H) was detected in both tumor tissue and corresponding non-tumor tissue by WES, but the wild-type gene was determined in the corresponding non-tumor tissue by Sanger sequencing. In addition, protein-truncating genetic variants included frameshift indel mutation in ELF3 (c.909dupC:p.F303fs) and nonsense mutations in DOCK3 (c.C2483A:p.S828X) and KMT2C (c.C1519T:p.Q507X) were detected in tumor samples by Sanger sequencing (Fig. 3D). The Circos map visually summarized the somatic genomic variations of SNVs, INDEL and CNVs of the HMEC (*Supplementary Fig. 2*).

Bioinformatic

A total of 1004 significant mutated genes (source: Onco KB) in SNVs from 8 studies contained 1487 HCC patients (supplementary Fig. 3A) and 654 significant mutated genes (source: Onco KB) in SNVs from 7 studies contained 445 CHL patients were downloaded (supplementary Fig. 3B) (www.cbioportal.org). We also obtained 312 significant mutated genes in SNVs from 18 SMEC patients from Kang T *et al* study. There were six SNVs (STAT1, TGFBR1, NOTCH1, KMT2C, ELF3, GNAS) in the HMEC that overlapped with primary liver tumors (HCC and CHL), only CHD3 gene in HMEC that overlapped with SMEC (Fig. 3A). Especially, Somatic GNAS gene (included missense mutation, amplification, truncating mutation) altered in 2.1% (9/445) patients with primary hepatobiliary tumors included intrahepatic cholangiocarcinoma, extrahepatic cholangiocarcinoma and perihilar cholangiocarcinoma (Fig. 3B). In total of 3 patients underwent GNAS (p.R201H/C) missense mutation (putative driver) in exon8. Importantly, Sample ID (W012, T026) were *Opisthorchis viverrini*-associated with cholangiocarcinoma (SRP007970) (Fig. 3C).

Germline variants in the proband and pedigree analysis

The 56 germline variants in 20 Fanconi's anemia pathway genes included 19 missense variants and 25 synonymous variants and 12 UTR3 and UTR5 in the proband's corresponding non-tumor tissue by WES (Supplementary table 2). A total of five germline homozygous variants and six germline heterozygous variants in six Fanconi's anemia pathway genes (FANCA, FANCI, FANCW/RFWD3, FANCD1/BRCA2, FANCI/BRIP1, FAN1) were identified in the proband's non-tumor tissue by Sanger sequencing (Table 2, Fig. 4A).

Table 2
The sanger sequencing of germline variants in proband and family members

Gene	Locus	HGVS nomenclature	Alt	Rff	Proband	Sibling	Sibling	Son	Daughter
					64y	70y	61y	39y	41y
FANCI	15q26.1	exon4:c.C257T:p.A86V	CT	C	heterozygous	Non	Non	Non	Non
		exon22:c.G2225C:p.C742S	CG	C	heterozygous	Non	Non	Non	Non
FAN1	15q13.2	exon2:c.G698A:p.G233E	GA	G	heterozygous	heterozygous	heterozygous	Non	Non
FANCI/BRIP1	17q23.2	exon19:c.T2755C:p.S919P	TC	T	heterozygous	homozygous	homozygous	homozygous	homozygous
FANCA	16q24.3	exon16:c.G1501A:p.G501S	CT	C	heterozygous	homozygous	homozygous	homozygous	homozygous
		exon9:c.A796G:p.T266A	TC	T	heterozygous	homozygous	homozygous	homozygous	homozygous
		exon26:c.G2426A:p.G809D	TT	C	homozygous	homozygous	homozygous	homozygous	homozygous
FANCW/RFWD3	16q23.1	exon10:c.A1690G:p.I564V	CC	T	homozygous	homozygous	homozygous	homozygous	homozygous
		exon2:c.C269A:p.T90N	TT	G	homozygous	homozygous	homozygous	homozygous	homozygous
FANCD1/BRCA2	13q13.1	exon14:c.T7397C:p.V2466A	GG	A	homozygous	homozygous	homozygous	homozygous	homozygous
C17orf70	17q25.3	exon8:c.A2449G:p.T817A	CC	T	homozygous	homozygous	homozygous	homozygous	homozygous

There was no family history of Fanconi's anemia and solid tumor. The proband's parents died of cardiovascular and cerebrovascular diseases 10 years ago. Only the old sibling showed hypertension and type 2 diabetes. The proband's offspring did not show any disease. The same mutational variants in FANCD1/BRCA2, FANCW/RFWD3, and FAN100/C17orf70 were verified in the pedigree. Heterozygous variants in FANCA (c.G1501A:p.G501S), FANCA (c.A796G:p.T266A) and FANCI/BRIP1 (c.T2755C:p.S919P) were detected in the proband, but homozygous mutations were shown in the other family members. Heterozygous FAN1 variants were detected in the siblings and proband. Only heterozygous FANCI variants (c.C257T:p.A86V and c.G2225C:p.C742S) were unique in the proband (Table 2, Fig. 4B,C).

Discussion

The correlation between two rare diseases is really difficult for clinicians. The emergence of next-generation sequencing technologies has provided a simple and powerful approach for discovering de novo disease-associated genes, and these methods have furthered our understanding of the rare HMEC, which lacked the traditional high risk factors such as hepatitis B, hepatitis C, long-term alcohol intake history and cirrhosis, like most primary HMEC cases reported in the literatures (Table 1). In 2006, Zhu *et al.* reported an adult male patient, also absent for high risk factors who was first diagnosed with unusual HCC metastatic to right proximal ulna and metachronous esophageal squamous cell carcinoma resulting from the history of Fanconi's anemia¹². Linares *et al* also report on a 31-year-old female patients with synchronous squamous cell carcinoma of esophagus and HCC associated with Fanconi's anemia¹³. However, the present case only showed mild anemia, with an absence of the typical Fanconi's anemia phenotype, only present of family Fanconi's anemia gene carriers. In fact, increasing evidence has suggested that monoallelic carriers for Fanconi's anemia genes were characterized by a adult-set predisposition to most solid cancers, especially squamous cell carcinomas from the epithelia of genitourinary tracts and the aerodigestive system¹⁴. A previous study by Alter *et al.* reported that 20–30% of germline Fanconi's anemia presents with unusual solid malignancies as the first clinic manifestation and shows absence of the phenotype of congenital Fanconi's anemia^{14, 15}. Interestingly, three patients were reported with HMEC, also absence of Fanconi's anemia, combined with synchronous hepatocellular carcinoma¹⁶, synchronous squamous cell carcinoma in the cranial skin¹⁷ and metachronous gastric malignant carcinoma¹⁸.

In fact, the phenotypes of germline Fanconi's anemia mutation-related solid tumors were probably determined in mutation loads or a dose-dependent manner¹⁴. So far, a total of 22 proteins (FANCA–FANCW/RFWD3 genes coding) and other FA network genes have been identified to function in Fanconi's

anemia pathway¹⁹. These proteins participate in pathways including genome maintenance processes and DNA repair in response to DNA damage, as well as interstrand cross-linking repair, homologous recombination and non-homologous terminal junctions²⁰. Compared with the 22 Fanconi's anemia genes, FAN1 has a mild role in interstrand crosslink repair and even patients with homozygous mutation in FAN1 were absent of Fanconi's anemia features. However, *Lachaud et al* showed that FAN1 defects can cause cancers in knockin mice, and also FAN1 variant in high-risk pancreatic cancers abolishes recruitment by Ub-FANCD2, resulted in genetic instability without affecting interstrand crosslink repair²¹. Otherwise germline FAN1 mutation, occurred frequently in high-risk pancreatic cancers²² and hereditary susceptibility to familial colorectal cancers²³. In the present case, we testified FAN1 mutations were present in the pedigree. Therefore, we propose that germline Fanconi's anemia mutations are probably predisposing factors to the occurrence of HMEC.

More importantly, Mutations in the GNAS gene typically occur at exon 8, in which Arg201 is converted to either a cysteine (R201C) or a histidine (R201H), lead to activation of the Gas subunit. This Gas constitutively activate the intracellular cyclin adenosine adenosine monophosphate (cAMP) signal pathway²⁴. Otherwise, GNAS R201H/C missense mutation have been showed a cross-communication between JAK/STAT and cyclic-AMP pathways in rare subtypes of liver inflammatory tumorigenesis²⁵. Farges et al. also described an adult male patient with inflammatory hepatic adenoma associated with Fanconi's anemia and somatic GNAS mutation who developed malignant transformation of HCC²⁶. Consistent with inflammatory phenotype in the present HMEC, previous studies reported three HMEC patients with inflammation phenotype and inflammatory cell infiltration in the corresponding tumor-free liver tissue²⁶. Otherwise, somatic GNAS R201H/C mutation occurs frequently in secreting-mucous tumors like pancreatic intraductal papillary mucinous neoplasms (IPMN) as a bona fide precursor to carcinogenesis²⁹. GNAS R201 mutation was detected in pancreatic IPMN tissue, secretin-stimulated pancreatic juice and peripheral blood³⁰. The mucus production and carcinogenesis of the intestinal subtype of intraductal papillary neoplasm of the biliary ducts (IPNB), a counterpart of pancreatic IPMN, have also been connected with gain-of-function mutations of GNAS R201³¹. Otherwise, The protein-truncating genetic variants in the present case included a frameshift insertion in ELF3 and nonsense mutation in KMT2C, which were also reported in biliary tumors as tumor suppressors, with consistently positive immunohistochemical results for CK7 and CK19 in the present case, which may suggest the possibility that HMEC originates from the biliary system³². Moreover, GNAS and KMT2C were almost only mutated in O.viverrini-CHL compared non-O.viverrini-CHL, which consistent with Jarley K et.al study that three HMEC patients were induced by biliary parasite infection³³. and may explained that most HMECs(20/23) were reported in Asia areas with a high incidence of parasites (Table 2).

In conclusion, the molecular characteristics of the current HMEC were more similar to primary liver biliary tumors rather than to SMEC. We present here for the first time the etiology of HMEC associated with germline Fanconi's anemia mutations and somatic GNAS R201 mutation.

Abbreviations

MEC: Mucoepidermoid carcinoma, HMEC: hepatic mucoepidermoid carcinoma, SMEC: salivary gland mucoepidermoid carcinoma, HCC: hepatocellular carcinoma, CHL: cholangiocarcinoma, IPMN: intraductal papillary mucinous neoplasms, IPNB: intraductal papillary neoplasm of the biliary ducts, SNV: single-nucleotide variant, CNV: copy number variant. WES: whole-exome sequencing. Non: not have Np: not provided, RL: right liver, LL: left liver, BD: bile duct, GB: gallbladder, S: surgery, R: Radiotherapy, C: Chemotherapy, Con: Conservative treatment, TACE: transcatheter arterial chemoembolization. PTCD: percutaneous transhepatic cholangial drainage. OS: overall survival.

Declarations

Acknowledgements

We thank the generosity of the patient and his family, We would also like to thank Novogene Co., Ltd and BGI TECH SOLUTIONS (BEIJING LIUHE) CO. LIMITED for DNA sequencing services. we also thank Feng Zhang, PhD, from the Institute of Translational Medicine, Nanchang University for professional knowledge guidance in sequencing.

Author contributions

Ping Hou and Xiaoyan Su who are the first co-author, contributed equally to the study. This study was designed by Wenjun Liao and Linqun Wu. Manuscript was written by Ping Hou and Xiaoyan Su. Pedigree analysis and clinical phenotype analysis was performed by Jiakun Wang and Zhihao Huang. with further review by Lixiang Li, Xiaoyan Su and Liping Xu. Whole exome sequencing and bioinformatic analysis by Wei Cao, Jiakun Wang, Rongguiyi Zhang, Zhihao Huang.

Funding

This work was supported by CHEN XIAO-PING FOUNDATION FOR THE DEVELOPMENT OF SCIENCE AND TECHNOLOGY.

Ethics approval and consent to participate

This study was approved by the Ethics Committee of the Second Affiliated Hospital of Nanchang University, and informed consent was obtained from the patient and his family.

Disclosed of potential conflicts of interest

The authors declare no conflict of interests. The authors declare no competing financial interest.

Consent for publication

Not applicable.

Competing interests

The authors declare no competing financial interests.

References

1. Nallacheruvu Y, Gaur K, Sakhuja P, Agarwal AK, Srivastava S. Mucoepidermoid Carcinoma of the Gallbladder: A Case-Based Study of an Extremely Rare Tumor Highlighting the Role of Immunohistochemical Profiling. *INT J SURG PATHOL*. 2019;27:418-422.
2. Tonon G, Modi S, Wu L, et al. t(11;19)(q21;p13) translocation in mucoepidermoid carcinoma creates a novel fusion product that disrupts a Notch signaling pathway. *NAT GENET*. 2003;33:208-213.
3. Lennerz JK, Perry A, Mills JC, Huettner PC, Pfeifer JD. Mucoepidermoid carcinoma of the cervix: another tumor with the t(11;19)-associated CRTCC1-MAML2 gene fusion. *AM J SURG PATHOL*. 2009;33:835-843.
4. Achcar RDOD, Nikiforova MN, Dacic S, Nicholson AG, Yousem SA. Mammalian mastermind like 2 11q21 gene rearrangement in bronchopulmonary mucoepidermoid carcinoma. *HUM PATHOL*. 2009;40:854-860.
5. Saeki K, Ohishi Y, Matsuda R, et al. "Pancreatic Mucoepidermoid Carcinoma" Is not a Pancreatic Counterpart of CRTCC1/3-MAML2 Fusion Gene-related Mucoepidermoid Carcinoma of the Salivary Gland, and May More Appropriately be Termed Pancreatic Adenosquamous Carcinoma With Mucoepidermoid Carcinoma-like Features. *AM J SURG PATHOL*. 2018;42:1419-1428.
6. Watanabe J, Kai K, Tanikawa K, et al. Primary mucoepidermoid carcinoma of the liver with CRTCC1-MAML2 fusion: a case report. *DIAGN PATHOL*. 2019;14:84.
7. Moul AE, Bejarano PA, Casillas J, Levi JU, Garcia-Buitrago MT. Mucoepidermoid Carcinoma of the Intrapancreatic Common Bile Duct: Immunohistochemical Profile, Prognosis, and Review of the Literature. *Case Reports in Pathology*. 2013;2013:1-5.
8. Deeg HJ, Socie G, Schoch G, et al. Malignancies after marrow transplantation for aplastic anemia and fanconi anemia: a joint Seattle and Paris analysis of results in 700 patients. *BLOOD*. 1996;87:386-392.
9. Gao J, Aksoy BA, Dogrusoz U, et al. Integrative analysis of complex cancer genomics and clinical profiles using the cBioPortal. *SCI SIGNAL*. 2013;6:11.
10. Cerami E, Gao J, Dogrusoz U, et al. The cBio Cancer Genomics Portal: An Open Platform for Exploring Multidimensional Cancer Genomics Data: Figure 1. *CANCER DISCOV*. 2012;2:401-404.
11. Kang H, Tan M, Bishop JA, et al. Whole-Exome Sequencing of Salivary Gland Mucoepidermoid Carcinoma. *CLIN CANCER RES*. 2017;23:283-288.
12. Zhu AX, D'Andrea AD, Sahani DV, Hasserjian RP. Case 13-2006: A 50-Year-Old Man with a Painful Bone Mass and Lesions in the Liver. *The New England Journal of Medicine*. 2006;354:1828-1837.
13. Linares M, Pastor E, Gomez A, Grau E. Hepatocellular carcinoma and squamous cell carcinoma in a patient with Fanconi's anemia. *ANN HEMATOL*. 1991;63:54-55.
14. Nalepa G, Clapp DW. Fanconi anaemia and cancer: an intricate relationship. *NAT REV CANCER*. 2018;18:168-185.
15. Alter BP, Greene MH, Velazquez I, Rosenberg PS. Cancer in Fanconi anemia. *BLOOD*. 2003;101:2072.
16. Kang H, Park YN, Kim SE, et al. Double primary mucoepidermoid carcinoma and hepatocellular carcinoma of the liver—a case report. *Hepatogastroenterology*. 2003;50:238-241.
17. Nishiyama M, Mizukami Y, Kume M, et al. [Mucoepidermoid carcinoma of the intrahepatic bile duct with metastasis to the cranial skin]. *Nihon Shokakibyō Gakkai Zasshi*. 2012;109:1953-1959.
18. Hayashi I, Tomoda H, Tanimoto M, et al. Mucoepidermoid carcinoma arising from a preexisting cyst of the liver. *J SURG ONCOL*. 1987;36:122-125.
19. Nepal M, Che R, Zhang J, Ma C, Fei P. Fanconi Anemia Signaling and Cancer. *Trends in Cancer*. 2017;3:840-856.
20. Wang AT, Smogorzewska A. SnapShot: Fanconi Anemia and Associated Proteins. *CELL*. 2015;160:354.
21. Lachaud C, Moreno A, Marchesi F, Toth R, Blow JJ, Rouse J. Ubiquitinated Fancd2 recruits Fan1 to stalled replication forks to prevent genome instability. *SCIENCE*. 2016;351:846-849.
22. Smith AL, Alirezaie N, Connor A, et al. Candidate DNA repair susceptibility genes identified by exome sequencing in high-risk pancreatic cancer. *CANCER LETT*. 2016;370:302-312.
23. Segui N, Mina LB, Lazaro C, et al. Germline Mutations in FAN1 Cause Hereditary Colorectal Cancer by Impairing DNA Repair. *GASTROENTEROLOGY*. 2015;149:563-566.
24. O'Hayre M, Vázquez-Prado J, Kufareva I, et al. The emerging mutational landscape of G proteins and G-protein-coupled receptors in cancer. *NAT REV CANCER*. 2013;13:412-424.
25. Nault JC, Fabre M, Couchy G, et al. GNAS-activating mutations define a rare subgroup of inflammatory liver tumors characterized by STAT3 activation. *J HEPATOL*. 2012;56:184-191.
26. Farges O, Ferreira N, Dokmak S, Belghiti J, Bedossa P, Paradis V. Changing trends in malignant transformation of hepatocellular adenoma. *GUT*. 2010;60:85-89.
27. Di Palma S, Andreola S, Audisio RA, Doci R, Lombardi L. Primary mucoepidermoid carcinoma of the liver. A case report. *Tumori*. 1992;78:65-68.
28. Katsuda S, Nakanishi I, Kajikawa K, Takabatake S. Mucoepidermoid carcinoma of the liver. *Acta Pathol Jpn*. 1984;34:153-157.

29. Patra KC, Kato Y, Mizukami Y, et al. Mutant GNAS drives pancreatic tumorigenesis by inducing PKA-mediated SIK suppression and reprogramming lipid metabolism. *NAT CELL BIOL.* 2018;20:811-822.
30. Berger AW, Schwerdel D, Costa IG, et al. Detection of Hot-Spot Mutations in Circulating Cell-Free DNA From Patients With Intraductal Papillary Mucinous Neoplasms of the Pancreas. *GASTROENTEROLOGY.* 2016;151:267-270.
31. Yang CY, Huang WJ, Tsai JH, et al. Targeted next-generation sequencing identifies distinct clinicopathologic and molecular entities of intraductal papillary neoplasms of the bile duct. *Mod Pathol.* 2019;32:1637-1645.
32. Nakamura H, Arai Y, Totoki Y, et al. Genomic spectra of biliary tract cancer. *NAT GENET.* 2015;47:1003-1010.
33. Koo J, Ho J, Wong J, Ong GB. Mucoepidermoid carcinoma of the bile duct. *ANN SURG.* 1982;196:140-148.

Figures

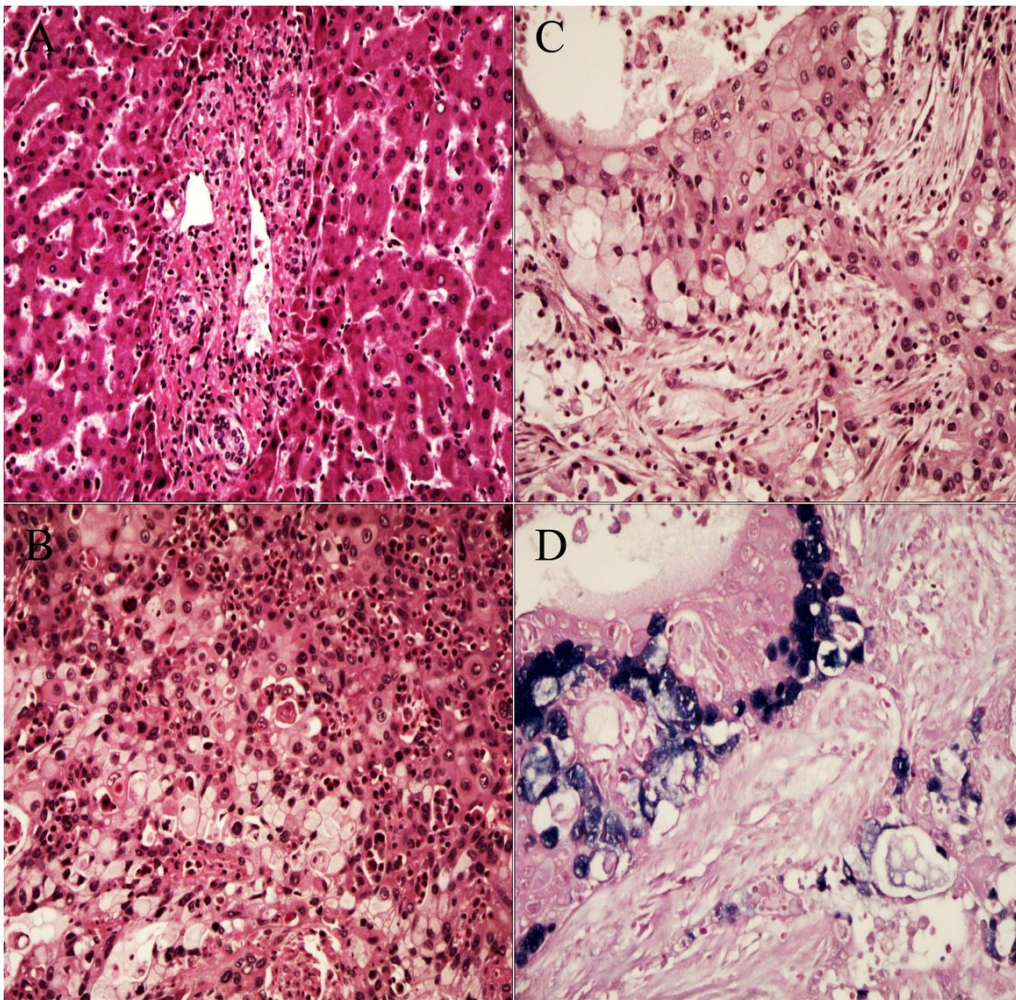


Figure 1
 Pathological results A. Dystrophic arteries and a large number of inflammatory cells, mainly included lymphocyte infiltrations, were observed in the portal area (H&E staining, magnification 100×) B. Eosinophil infiltrations were seen in the tumor area(H&E staining, magnification 200×) C. Hematoxylin and eosin (H&E) staining revealed malignant epidermoid cells and mucin-producing cells with intracytoplasmic mucin. The tumor cells infiltrated into the stroma with occasional keratinization (magnification 200×). D. Alcian blue stain-positive material highlights the mucin in mucin-producing cells (magnification 200×).

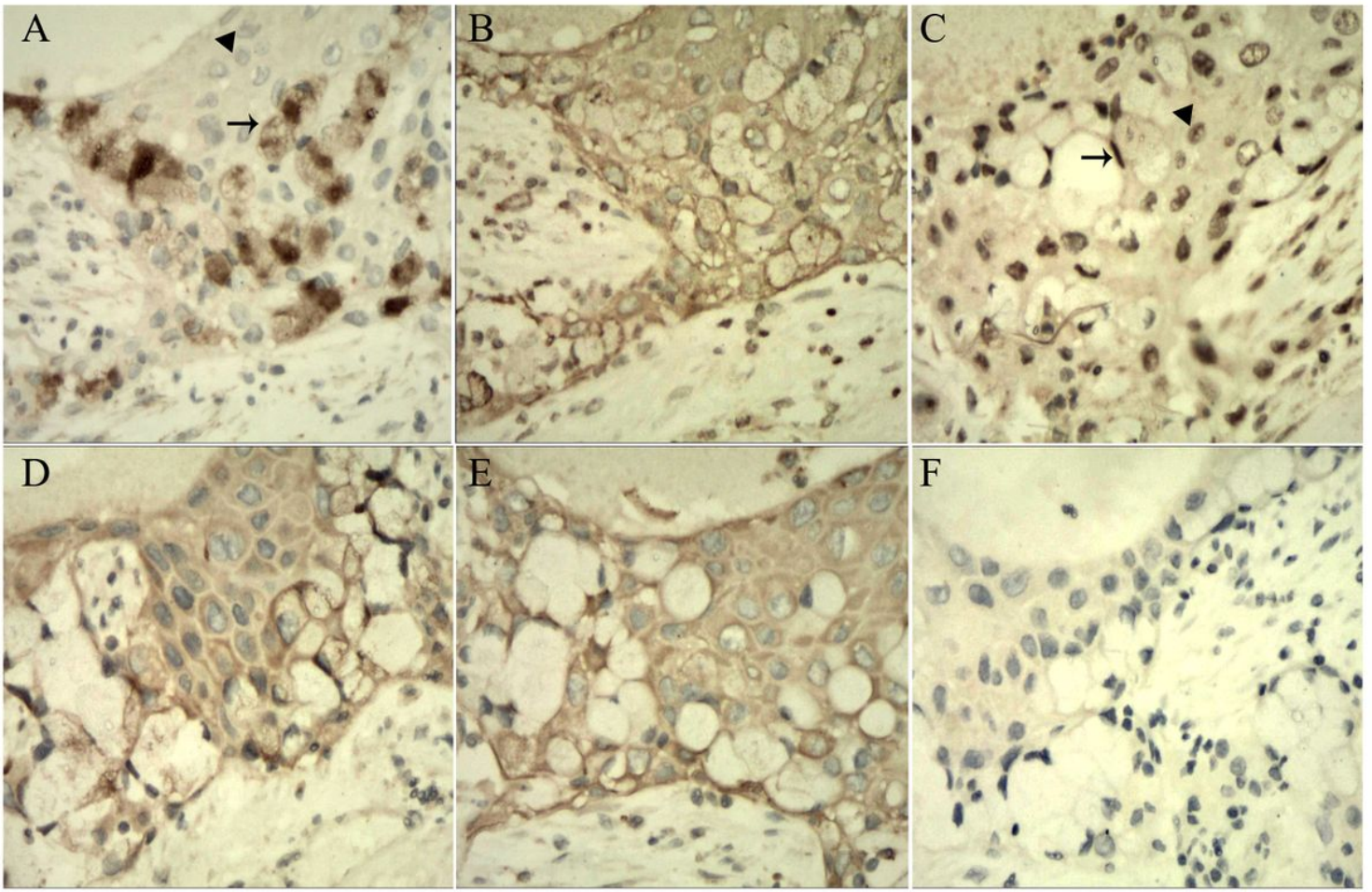


Figure 2

Immunohistochemical results A. Immunopositivity for cytoplasmic MUC5AC was detected the mucinous cells (long black arrow), with negative staining in epidermoid cells (magnification 200×). B. Immunopositivity for membrane MUC1 was detected in all epidermoid cells and mucinous cells (magnification 200×). C. Immunopositivity for p63 was detected in the nuclei of mucinous cells (long black arrow) and epidermoid cells (triangular arrow) (magnification 200×). D. The cytoplasmic CK19 stainings were focally positive in the epidermoid and mucious component of the tumor (magnification 200×). E. The cytoplasmic CK7 stainings were focally positive in the epidermoid and mucious component of the tumor (magnification 200×). F. Tumor cells were negative for membrane CEA staining (magnification 200×).

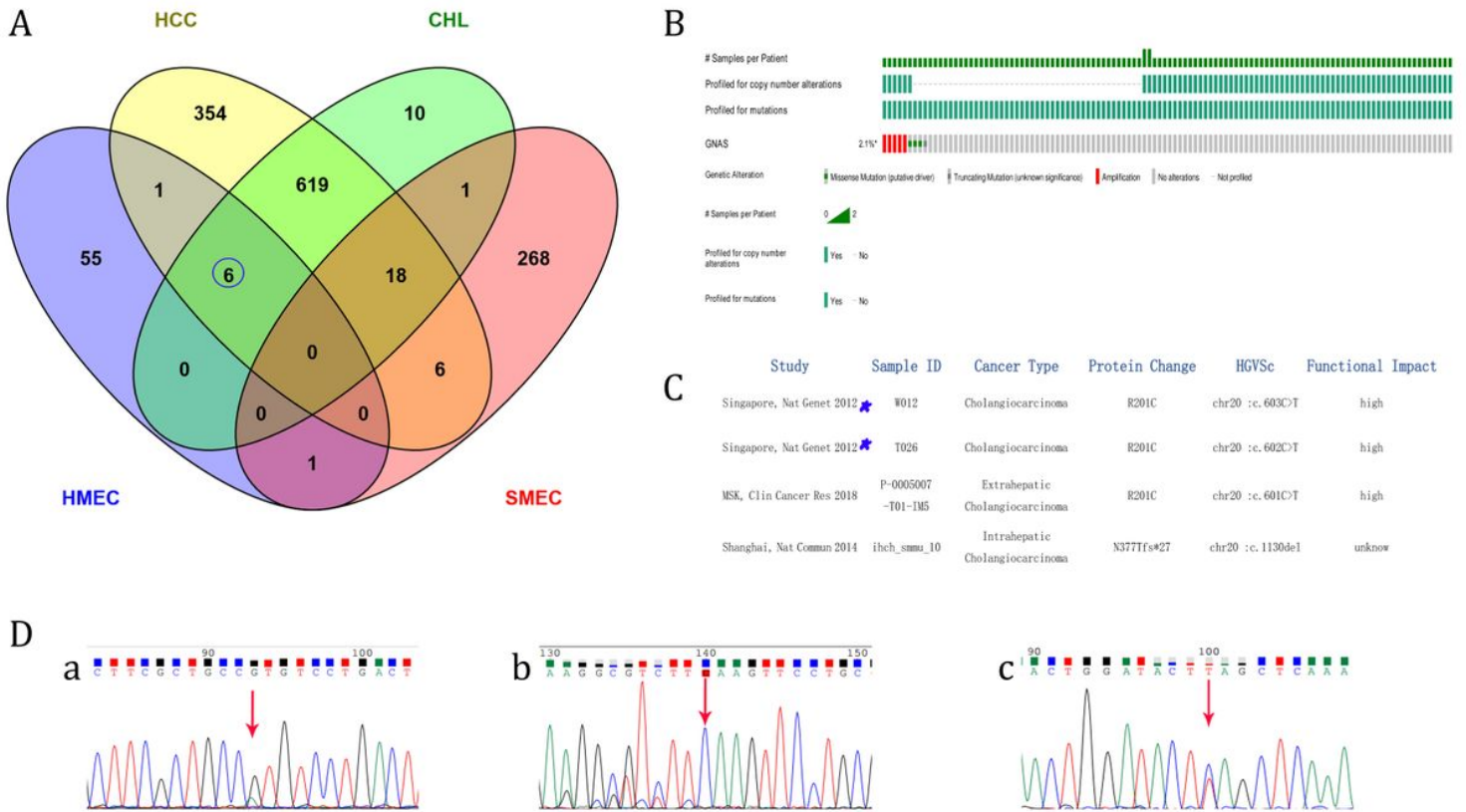


Figure 3

public data analysis and significant somatic mutation in proband. (Mutation diagram circles are colored with respect to the corresponding mutation types. In case of different mutation types at a single position, color of the circle is determined with respect to the most frequent mutation type). A. Venn diagram: six SNVs(STAT1,TGFBR1,NOTCH1,KMT2C,ELF3,GNAS) in the HMEC that overlapped with primary liver tumors (HCC and CHL),only CHD3 gene in HMEC that overlapped with SMEC.63 SNVs (non-synonymous mutation)in HMEC. B. Somatic GNAS gene mutation occurred in 2.1% (9/445) patients with primary hepatobiliary tumors via public databases. C. In total of 3 patients underwent GNAS (p.R201H/C) missense mutation(putative driver) .Samples (ID W012,T026) were *O.pisthorchis viverrini*-associated with cholangiocarcinoma (SRP007970)(pentagonal shape). D. Somatic mutations in proband by sanger sequencing a. missense variant GNAS (chr20.exon8:c.G602A:p.R201H),b. frameshift indel variant ELF3 (chr1,exon4:c.909dupC:p.F303fs), c. nonsense variant KMT2C (chr7,exon4:c.C1519T:p.Q507X) in tumor tissue.

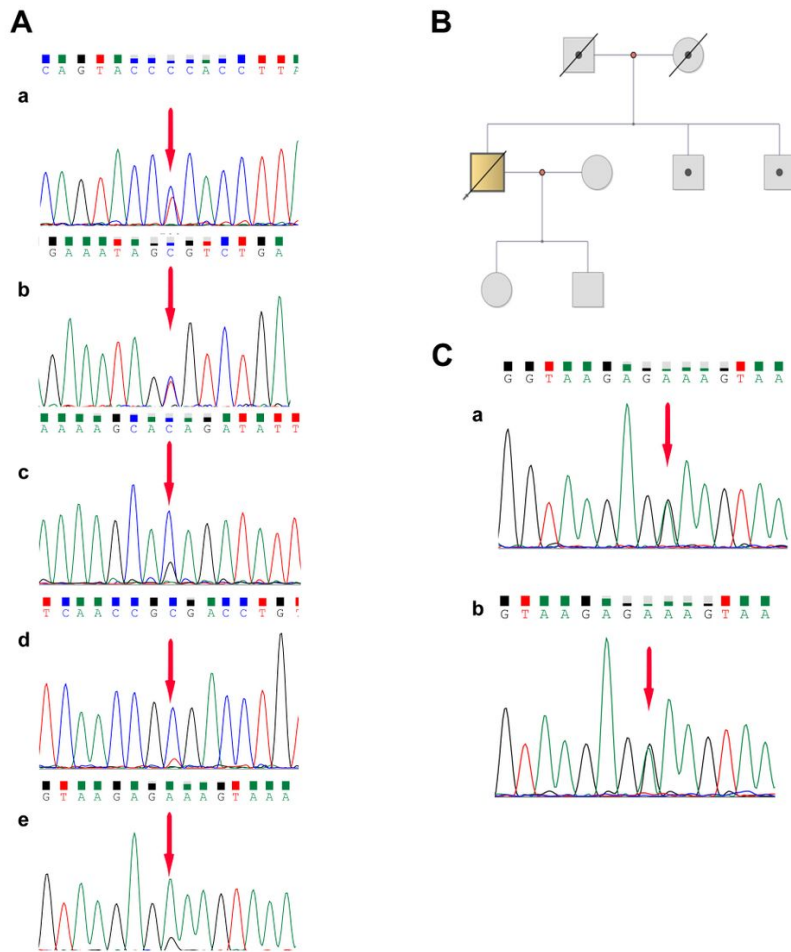


Figure 4
 Germline heterozygous mutations in the proband and pedigree screening A. a.FANCI(chr15.exon4:c.C257T:p.A86V)
 ;b.FANCI(chr15.exon22:c.G2225C:p.C742S);c.FANCI/BRIP1(chr17.exon19:c.T2755C:p.S919P),d.FANCA(chr16.exon9:c.A796G;p.T266A);e.FAN1(chr15.exon2:c.1698A:p.G233E)(corresponding non-tumor liver tissue) B. Pedigree map: the proband's parents died from cardiovascular and cerebrovascular diseases; there was no obvious Fanconi's anemia disease in the proband's offspring and brothers. C. Siblings A and B, FAN1 (exon2:c.G698A:p.G233E) (blood).

Supplementary Files

This is a list of supplementary files associated with this preprint. Click to download.

- [Supplementarymaterials.pdf](#)